J Mol Model (2011) 17:2465–2473
DOI 10.1007/s00894-010-0929-8

ORIGINAL PAPER

Prediction of zanamivir efficiency over the possible 2009 Influenza A (H1N1) mutants by multiple molecular dynamics simulations and free energy calculations

Dabo Pan · Huijun Sun · Chongliang Bai · Yulin Shen · Nengzhi Jin · Huanxiang Liu · Xiaojun Yao

Received: 5 October 2010 / Accepted: 6 December 2010 / Published online: 31 December 2010

Abstract As one of the most important antiviral drugs against 2009 influenza A (H1N1), will zanamivir be effective for the possible drug resistant mutants? To answer this question, we combined multiple molecular dynamics simulations and molecular mechanics generalized Born surface area (MM-GBSA) calculations to study the efficiency of zanamivir over the most frequent drug-resistant strains of neuraminidase including R293K, R152K, E119A/D and H275Y mutants. The calculated results indicate that the modeled mutants of the 2009-H1N1 strains except H275Y will be significantly resistant to zanamivir. The resistance to zanamivir is mainly caused by the loss of polar interactions. The identified potential resistance sites in this study will be useful for the development of new effective anti-influenza drugs and to avoid the occurrence of the state without effective drugs to new mutant influenza strains.

Keywords Drug resistance · 2009 H1N1 Influenza A virus · Molecular dynamics simulation · Molecular mechanics generalized Born surface area (MM-GBSA) · Zanamivir

D. Pan · C. Bai · H. Liu (✉)
School of Pharmacy, Lanzhou University,
Lanzhou 730000, China
e-mail: hxliu@lzu.edu.cn

H. Sun · H. Liu · X. Yao
State Key Laboratory of Applied Organic Chemistry
and Department of Chemistry, Lanzhou University,
Lanzhou 730000, China

Y. Shen · N. Jin
Gansu Computing Center,
Lanzhou 730030, China

Introduction

The high speed global spread of 2009 influenza A (H1N1) virus has given serious threat to the life of the general population all over the world. This new subtype A/H1N1 is a re-combined virus by human, swine, and avian influenza viruses with a high transmissible ability among human beings [1]. This new strain confers resistance to M2 channel inhibitors amantadine (AMT) and rimantadine (RMT) [2]. Fortunately, the neuraminidase (NA) inhibitors oseltamivir and zanamivir are still effective against the new virus. However, as these drugs are widely used, neuraminidase will face a selection pressure and possible mutants will occur. Some of these mutants will cause resistance to corresponding drugs. Once the drug-resistant strains occur, they will probably lead to a large scale outbreak of novel pandemic flu and cause an increase of the global public health concerns. Faced to the possible serious circumstance and future pandemic caused by drug resistance, it will be very useful if we can know the potential drug resistance sites of the effective neuraminidase inhibitors in advance. The information about the potential drug resistance sites can provide some insights to design new effective medicine against the possible drug resistant influenza strains. It would also be very significant to avoid the occurrence of the state without effective drugs to new mutant influenza strains.

Subtype-specific NA mutations conferring resistance to NA inhibitors have been reported by in vitro experiments and clinical cases. For example, the mutated framework residues H274Y and N294S are regularly identified in N1. For the N2 and N9 subtypes, two mutations of the binding residues (E119V and R292K) for oseltamivir were detected after treatment of the infected patients with oseltamivir [3–8]. Several neuraminidase mutants E119G/A/V/D, R292K

and R152K in the N2 and N9 subtypes confer resistance to zanamivir [8, 9]. Do these drug resistance mutants occur in 2009 influenza A (H1N1) virus? Actually, as oseltamivir is widely used to treat the patients infected with pandemic (H1N1) 2009 virus, the new influenza strain including H275Y (numbered according to H1N1 sequence) mutation has been separated in clinical recently [10]. However, once the drug resistance strain occurs in clinical, it will result in the situation without effective drugs. Thus, it is necessary to identify the potential drug resistance sites in advance. Compared with the experimental methods to identify the potential drug resistance sites, molecular modeling method has some advantages: it is easy to implement and can give reasonable results; it is not restricted by laboratory condition. Recently, molecular dynamics (MD) simulation combined with binding free energy calculation has been developed to investigate the molecular mechanism of drug resistance and evaluate the potency of an inhibitor to combat resistance [11–14]. Among the molecular dynamics simulation-based approaches, a commonly used and tractable approach for binding free energy calculation is the molecular mechanics Poisson–Boltzmann surface area (MM-PBSA) method [15, 16]. Recently, there has been an increased interest in the faster molecular mechanics generalized Born surface area (MM-GBSA) variant of MM-PBSA, which replaces the PB electrostatics with the generalized Born (GB) approximate model of electrostatics in water [15, 17, 18]. Although MM-PBSA is widely used, MM-GBSA method has been demonstrated to be sometimes more efficient than MM-PBSA in the study of the macromolecule-ligand interaction [19–21].

In our previous work, we applied in silico method to identify the potential drug resistant sites of 2009 influenza A (H1N1) virus neuraminidase based on single trajectory molecular dynamics (MD) simulation combined with binding free energy calculation [22]. This method is fast and effective. However, it can just identify the potential residue mutations with direct interaction to the inhibitors. It can not be applied to the mutations away from the active site. Compared with single trajectory molecular dynamics (MD) simulation, multiple trajectories method generally can give a more accurate result and can be used to study the effect of mutations both for the residues in the binding site and away from the binding site at much higher precision. Recently, Rungrotmongkol et al. applied multiple trajectories molecular dynamics (MD) simulation combined with linear interaction energy (LIE) method to predict oseltamivir efficiency against possible influenza A (H1N1-2009) mutants, suggesting several mutations confer to the oseltamivir resistance [23]. However, LIE method is an empirical method and needs the experimental binding free energy of several inhibitors or several mutations to obtain the involved parameters of the equation. For influenza A (H1N1-2009) neuraminidase, there is no enough experimental data to obtain reliable parameters of LIE equation. In addition, they just studied the oseltamivir efficiency against probable influenza A (H1N1-2009) mutants. For another important antiviral drug zanamivir, we still lack relevant information about its efficiency.

To predict the efficiency of zanamivir over the possible mutant strains of the 2009-H1N1 influenza, MD simulations combined with MM-GBSA were performed on the complexes of zanamivir bound to 2009-H1N1-mutated neuraminidase strains with R293K, R152K, E119A/D and H275Y mutations, respectively (the involved residues are displayed in Fig. 1). By comparing the binding free energy and the structural features of zanamivir to wild type and mutated neuraminidase, the potential drug resistant mutations and the correlated mechanism were discussed.

Materials and methods

The wild type complex of zanamivir bound to homology modeled A/H1N1-NA was obtained from our recent publication [22]. The mutated neuraminidase strains with the R293K, R152K, E119A/D and H275Y substitutions were obtained by using the wild type complex as the initial structure and changing the specific residues by Pymol program [24]. During the review progress of our manuscript, the wild type H1N1 neuraminidase crystal structure without ligand was obtained (pdb code 3NSS) [25]. By comparing our structure obtained from homology modeling and the recent reported crystal structure, we found they were very similar, indicating our homology modeling and molecular simulation are reasonable.

The wild type and mutated complex structures were further treated and used as the initial structures for molecular dynamics simulation. The main procedure for the structure treatment included the addition of hydrogen atoms and eight disulfide bonds for protein using the leap module together with the parameterization of receptor and ligands in AMBER 10.0 software package [26]. The standard AMBER force field for bio-organic systems (ff03) [27–29] was used to describe the neuraminidase parameters. The partial charges and force field parameters of zanamivir were taken from our previous study [22]. For each system, the counter ions were added to neutralize each ligand-bound system. Then, the corresponding systems were solvated using atomistic TIP3P water [30] in a octahedron box with at least 10 Å distance around the complex.

The molecular dynamics simulations including energy minimization and equilibration protocols were performed by using AMBER 10.0 software package [26]. The energy minimization was first conducted using the steepest descent

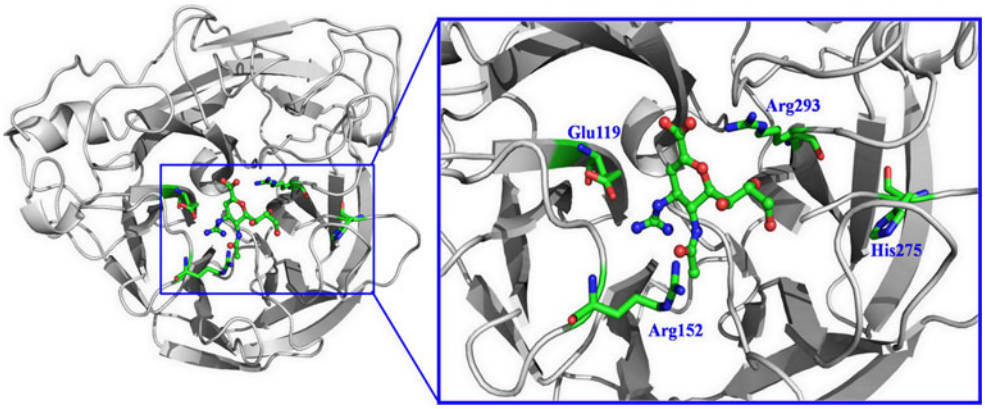

Fig. 1 The studied complex of zanamivir and neuraminidase (the involved mutations were displayed in sticks)

method switched to conjugate gradient every 1000 steps for a total of 2000 steps. As follows, the system was annealed from 0 to 300 K over a period of 50 ps using a Langevin thermostat with a coupling coefficient of 2.0/ps. All subsequent stages were carried out in the isothermal isobaric (NPT) ensemble using a Berendsen barostat [31] with a target pressure of 1 bar and a pressure coupling constant of 2.0 ps. The systems were again equilibrated for 500 ps. The production phase of the simulation was run by maintaining the 0.1 kcal mol^{-1} $Å^{-2}$ force constants on the restrained atoms for a total of 10 ns. Here, in the 10 ns production phase, the restrained atoms included the heavy atoms of the residues 95-216 and 449-467, which lie in the close contact surface of each monomer. The aim to restrain these residues is to keep the backbone fold intact like the natural tetramer since we used the monomer during molecular dynamics. During the whole simulation processes, long-range Coulombic interactions were handled using the particle mesh Ewald (PME) summation [32]. For the equilibration and production run, the SHAKE algorithm [33] was employed on all atoms covalently bonded to a hydrogen atom, allowing for an integration time step of 2 fs.

Following the MD process, MM-GBSA calculations were performed using AMBER10 [26] to compare the binding energy of zanamivir to wild type and mutated strains. The first step of MM-GBSA method is the generation of multiple snapshots from an MD trajectory of the protein-ligand complex, stripped of water molecules and counter ions. Snapshots, equally spaced at 10 ps intervals, were extracted from the MD production equilibrated trajectory. For each snapshot, the free energy is calculated for each molecular species (complex, protein, and ligand). The binding free energy is computed as the difference:

$$\Delta G_{bind} = G_{complex} - G_{protein} - G_{ligand} \quad (1)$$

The free energy G for each species can be calculated by the following scheme using the MM-GBSA method [19, 20]:

$$G = E_{gas} + G_{sol} - TS \quad (2)$$

where E_{gas} is the gas-phase energy; G_{sol} is the solvation free energy which (or and it) can be decomposed into polar and nonpolar contributions. T and S are the temperature and the total solute entropy, respectively.

In amber force field, the gas-phase energy includes the bond, angle, and torsion energies as well as the Coulomb and van der Waals energies [29]. In MM-GBSA method, the solvation free energy can be calculated as follows,

$$G_{sol} = G_{GB} + G_{nonpolar} \quad (3)$$

$$G_{nopolar} = \gamma SASA + b. \quad (4)$$

Here, G_{GB} is the polar solvation contribution calculated by solving the GB equation [19, 20]. Dielectric constants for solute and solvent were set to 4 and 80, respectively. $G_{nonpolar}$ is the nonpolar solvation contribution and was estimated by the solvent accessible surface area (SASA) determined using a water probe radius of 1.4 Å. The surface tension constant γ was set to 0.0072 kcal mol^{-1} $Å^{-2}$ and b was set to 0 kcal mol^{-1} [34].

The vibrational entropy contributions are estimated by normal mode analysis [35]. Because of the high computational demand, only 20 snapshots were used in normal mode analysis for every trajectory and each snapshot was optimized for 100,000 steps using a distance-dependent dielectric of $4r_{ij}$ (r_{ij} is the distance between atoms i and j) until the root-mean-square deviation of the gradient vector was less than 0.0001 kcal mol^{-1} $Å^{-2}$.

Results and discussion

Simulation stability

For each system, 10 ns molecular dynamics production simulation was performed. Here, the equilibration of the MD trajectories was monitored from the convergence of the root-mean square deviation (RMSD) of Cα atoms as well

as the time evolution of RMSD of Cα atoms for the residues in 5 Å around ligand and RMSD of heavy atoms for ligand for each system from the original starting coordinates (Fig. 2a-c). By monitoring the RMSD of Cα atoms of the whole protein, most systems have a similar trend and are up to equilibration in the last two nanoseconds. From the time evolution of RMSD of Cα atoms for the residues in active site, R293K strain, relative to other systems, has a larger structural fluctuation. The RMSD change of heavy atoms for ligand indicates several mutations including R293K, E119D and R152K will influence the binding mode of ligand and make zanamivir binding less stable.

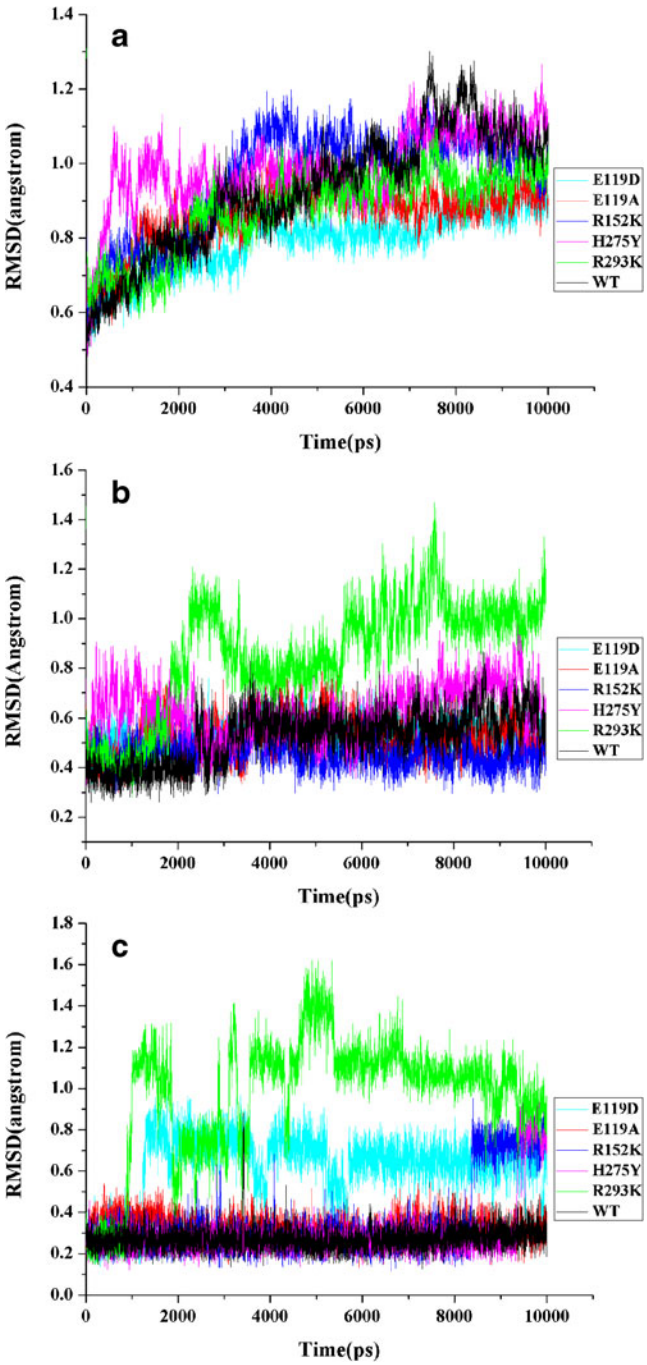

Fig. 2 The monitoring of the equilibration for the MD trajectories: (**a**) The time series of the RMSD of Cα atoms from the initial structure; (**b**) Time evolution of RMSD of Cα atoms for the residues around 5 Å of the ligand; (**c**) Time evolution of the RMSD of heavy atoms for the ligands

How do their mutations influence the ligand binding? In Figs. 3 and 4, we analyzed the hydrogen bond features between zanamivir and protein for wild type and mutation types. Here, the default geometric criterion to define the hydrogen bond is used: the donor-acceptor heavy atom distance should be less than 3.5 Å, and the donor-hydrogen-acceptor angle should be larger than 120°. For the wild type strain, from Fig. 4a, several pairs of important hydrogen bonds were formed. For example, the carboxyl group of zanamivir as hydrogen bond acceptor formed the conserved hydrogen bonds with three residues including R118, R293 and R368. There are several hydrogen bond pairs between the guanidinyl group and the residues with negative charge such as E119, E228 and E278. For the amide group of zanamivir, two pairs of hydrogen bonds are formed with R152 and E278. In addition, the 1,2,3-trihydroxy propyl group (-CH(OH)CH(OH)CH_2(OH)) formed the hydrogen bonds with two residues E277 and N295. From Figs. 3 and 4, it can be seen that the R293K mutation reduces the formation of hydrogen bonds largely. Several important hydrogen bonds including pairs between the carboxyl group and R293 as well as R368, between amide group and E278, between the 1,2,3-trihydroxy propyl group and N295 disappear completely. The disappearing of several hydrogen bonds between zanamivir and protein should be responsible for the large RMSD of ligand and active site of neuraminidase. Surprisingly, these large structural changes are not in agreement with the result from X-ray structures of the highly homologous N9 neuraminidase [36, 37]. According to the reported X-ray structures of N9 neuraminidase, R293K replacement only made a very local structural change. To find why our studied H1N1 neuraminidase has a large structural change upon the R293K mutation, first we compared the difference of the H1N1 and N9 neuraminidase. By comparing the the H1N1 and N9 neuraminidase structures, we found one loop (344-347) around Arg293 and Arg368 (according to H1N1 sequence number) was very different in the sequence and the corresponding conformation (shown in Fig. 5). In N9 neuraminidase, this loop is composed of four asparagines. The two middle asparagines form a good packing with the neighboring loop residues Trp295 and Gln296, making the loop have a relative rigid conformation. The rigid conformation of the loop restrains the movement of Asn347 and the formation of the hydrogen bond between Asn347 and Lys293 or Arg368. However, in the H1N1 neuraminidase,

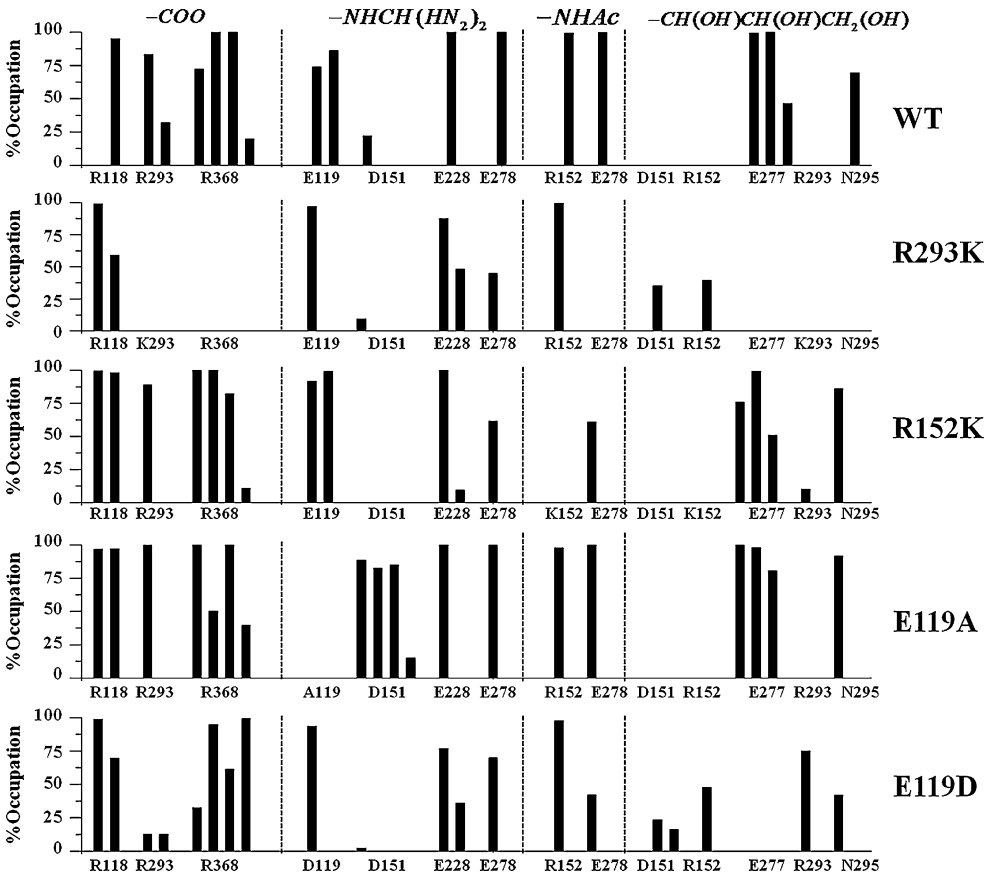

Fig. 3 Percentage occupation of hydrogen bonds between zanamivir and the NA residues in wild type and different mutants

the corresponding loop is composed of Asn344, Ala345, Gly346 and Asn347. The relative small residues replacing two middle asparagines result in the packing with the neighboring loop disappearing and make this loop more flexible. By monitoring molecular dynamics trajectories, we can see that residue Asn347 forms hydrogen bond either with the mutated Lys293 or Arg368 (Fig. 6). The formation of these hydrogen bonds may interrupt the interaction between Lys293 or Arg368 and zanamivir, making the large conformation rearrangement happen. Meanwhile, from the crystal structure of N9 neuraminidase with R293K mutation, it can be seen that two important water molecules entered into the active site around carboxyl group of inhibitors and the mutated K293. These two water molecules as a bridge play an important role to stabilize the local conformation, making the R293K mutation only result in a very small local change of structure compared with the wild type one. The missing of these crystallized water molecules around K293 and R368 in our homology modeled structure may also affect the arrangement of the corresponding residues and the binding mode of zanamivir.

Compared with R293K mutation, E119D and R152K mutations also reduce the formation of hydrogen bonds but with relative lighter degree compared with R293K mutation. E119D mutation changes the hydrogen bond occupation between the mutated residue 119 and guanidinyl group of zanamivir and makes the hydrogen bond pair between E227 and zanamivir vanishing. The decreasing of these hydrogen bond interactions affects the binding stability of zanamivir but does not affect the flexibility of active site for E119D mutants. Compared with wild type strain, only one hydrogen bond pair disappears in R152K mutation and thus makes a small effect on the zanamivir binding.

The identification of potential drug resistance sites from binding free energy calculation

To estimate the effect of the studied mutants on the binding free energy of zanamivir and to identify the potential drug resistance sites, a MM-GBSA analysis was performed using the extracted snapshots from the last 2 ns of the MD simulation. The calculated binding energies for zanamivir are given in Table 1. From Table 1, it can be seen that all the studied mutations except H275Y will weaken the interaction between neuraminidase and zanamivir. The H275Y mutant has a similar or even lower binding free energy with zanamivir compared to the wild type neuraminidase. The calculated results indicate that several mutations including R293K, E119D/A, D151A and R152K reduce the effectiveness of zanamivir and induce the occurrence of drug resistance. However, H275Y mutant which is a drug resistance mutation for oseltamivir will not induce the resistance of neuraminidase to zanamivir.

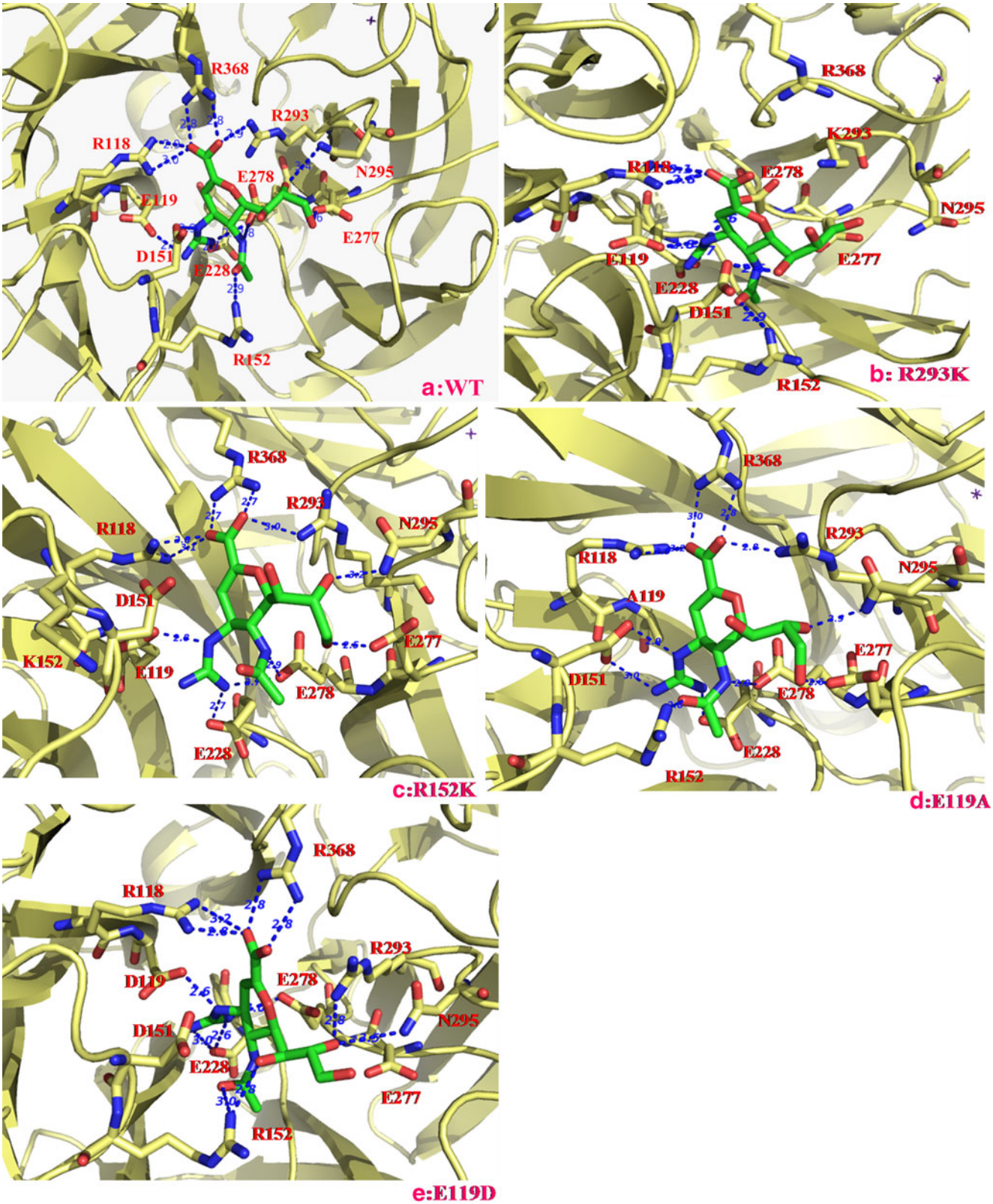

Fig. 4 The interaction between zanamivir and neuraminidase in wild type and different mutants

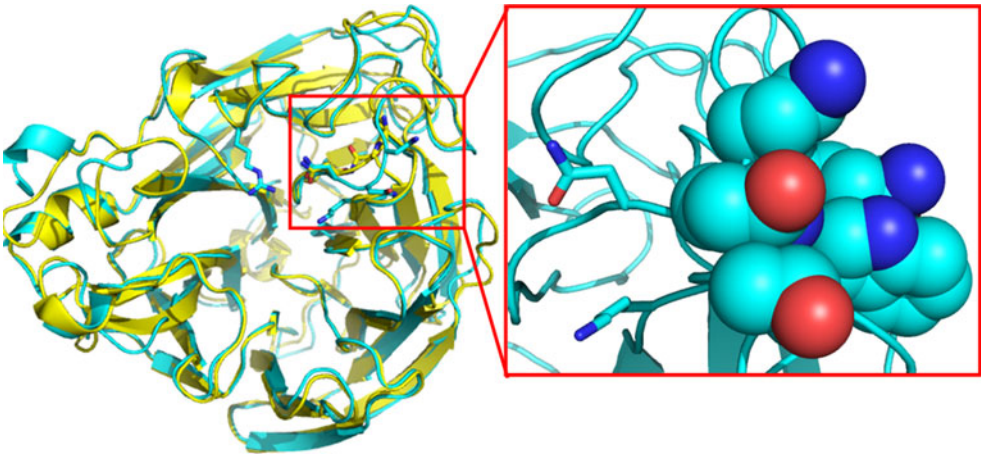

Fig. 5 The comparison of H1N1 and N9 neuraminidase structures (yellow: H1N1 neuraminidase; cyan: N9 neuraminidase with R293K mutation)

To display the loss degree of effectiveness, we further calculated the relative binding free energy ($\Delta\Delta G_{bind}$, is equal to $\Delta G_{mut} - \Delta G_{wt}$) of zanamivir over the studied mutants compared with wild type. The $\Delta\Delta G_{bind}$ for R293K, R152K, E119D, E119A are 13.65, 4.63, 4.47, 3.61 kcal/mol^{-1}, respectively. The reduction of binding free energy accounts for the descent of inhibitory activity of zanamivir to mutant strains. Overall, the modeled mutants of the 2009-H1N1 strains will be significantly resistant to zanamivir, with the ranked order of: R293K>R152K>E119D>E119A.

Although the potential drug resistance sites of neuraminidase of 2009 A/H1N1 to zanamivir are still unknown due to its limited use in clinical, we can not evaluate the accuracy of our results directly. But by comparing the reported drug resistance mutations for neuraminidase with other influenza strains to zanamivir and our calculated results, we can justify the reliability of our identified drug resistance sites indirectly.

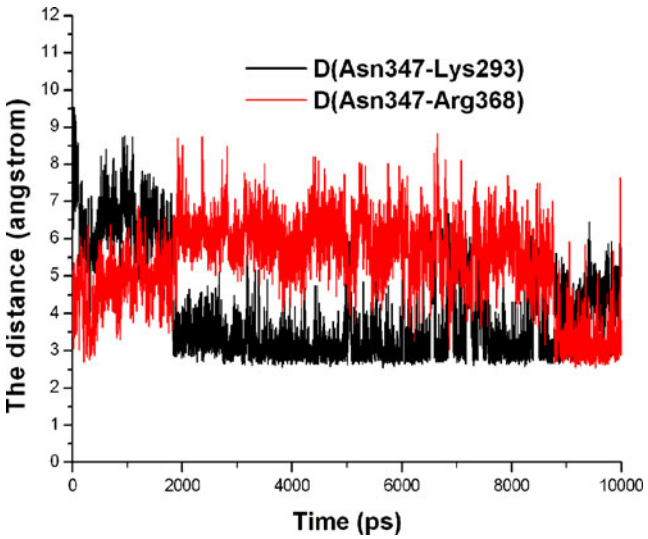

Fig. 6 The monitoring of the distance between the oxygen atom from side chain of Asn347 and the terminal nitrogen atom from side chain of Lys293 or Arg368

R293K strain has been reported to be resistant to zanamivir for several influenza strains such as H1N1/1933 and A/N2 [8, 9]. The resistance from E119A/D mutations to zanamivir was found in influenza A/N2 [9]. R152K strain was also found to be resistant to zanamivir in influenza B [9]. All these reported drug resistance sites in other influenza strains are identified to be resistant to influenza A/H1N1 neuraminidase in our calculations. Additionally, we also studied the effect of one oseltamivir-resistant mutation H275Y to the binding of zanamivir. The studied results indicate that this mutation does not influence the binding affinity of zanamivir, which is also consistent with the experimental results. For the drug resistance sites of neuraminidase to zanamivir, the H275Y mutation has never been reported. As for the rank of resistance potential, the studied mutants except R293K based on our calculation is basically consistent with the reported experimental binding affinity results for other influenza strains [9, 38]. For R293K mutants, the binding affinity may be underestimated due to the change of binding mode from the structural rearrangement of active site as discussed above and the improper estimation of binding free energy which will be discussed later.

In order to seek the origin to drive the loss of sensitivity of zanamivir to different mutants, we need to consider the interplay between the enthalpic and entropic contributions to binding free energy [39]. Enthalpic contributions provide a measure of the strength of the interactions between the inhibitor and the protein (electrostatic, van der Waals interactions), relative to those with the solvent. Entropic contributions comprise the change in solvent entropy arising from the burial of hydrophobic groups upon binding and the loss of solute conformational degrees of freedom (translational, rotational, and vibrational) [40]. By comparing the contribution of enthalpy of wild type and mutants, all potential drug resistance mutants have an unfavorable enthalpy contribution. From the perspective of entropy, three mutations E119A/D and R152K also display unfavorable effect for zanamivir binding compared with wild

Table 1 Binding free energies of zanamivir with different neuraminidase strains (kcal mol^{-1})

	ΔE_{int}^{ele}	ΔE_{int}^{vdw}	$\Delta G_{sol}^{nonpolar}$	ΔG_{sol}^{ele}	ΔG_{polar}	$\Delta G_{nonpolar}$	ΔH_{bind}	$-T\Delta S$	ΔG_{bind}
WT	-86.87	-18.49	-4.8	70.26	-16.61	-23.29	-39.89	23.83	-16.06
E119A	-81.63	-19.15	-5.03	67.02	-14.61	-24.18	-38.79	26.33	-12.46
E119D	-61.95	-22.95	-5.18	54.03	-7.92	-28.13	-36.05	24.46	-11.59
R152K	-73.26	-20.42	-4.79	60.61	-12.65	-25.21	-37.86	26.42	-11.44
H275Y	-79.36	-20.53	-4.87	64.27	-15.09	-25.4	-40.48	22.17	-18.31
R293K	-52.12	-15.42	-4.49	48.03	-4.09	-19.91	-23.99	21.58	-2.41

type. But the R293K mutant with the largest enthalpy loss has a favorable entropy contribution.

Furthermore, we decompose the enthalpy to be more detailed individual energy contribution to zanamivir binding in Table 1, including electrostatic and van der Waals energy contributions in gas phase, the polar and nonpolar solvation energy contributions. Generally, the electrostatic interaction contribution in gas phase is compensated by a large desolvation penalty which is polar solvation contribution. In order to identify the true electrostatic interaction contribution, we further decompose the binding free energy to polar and non-polar interaction contribution. The polar item composed of the electrostatic interaction in gas phase and the polar solvation contribution computed by solving the GB equation. The non-polar interaction was obtained by summing the van der Waals energy item and non-polar solvation contribution. From Table 1, the R293K mutation has the largest reduction in the binding ability to zanamivir. By analyzing the difference of every energy item contributed in wild type and R293K mutants, it can be seen that the loss of binding affinity mainly comes from the loss of polar interaction contribution. The replacement of R293 by lysine results in a decrease of more than 12 kcal mol^{-1} in the polar interaction contribution. This large decrease comes from a significant structural rearrangement and loss of important hydrogen bond interaction (Figs. 3 and 4) from one side. From another side, it may be from the inaccurate estimation of electrostatic interaction since it is still a challenge to estimate accurately the electrostatic interaction for binding free energy calculations. Thus, the inaccurate estimate of electrostatic interaction may also affect the reliability of binding free energy of R293K mutants. Besides the polar interaction contribution, the nonpolar interaction contribution also decreased more than 3 kcal mol^{-1}. The loss of nonpolar interaction contribution is from the packing loss of the side chain of R293 and zanamivir. From Fig. 4a and b, it can be seen that the substitution of R293 by lysine results in the complete loss of the interaction between this residue and zanamivir. For other mutants, from Table 1, the nonpolar interaction has a similar or larger contribution compared to wild type but the loss of polar interaction on a large degree results in the reduction of the total biding free energy furthermore resulting in the resistance to zanamivir. As shown in Fig. 4, the loss of polar interaction more or less depends on the change of hydrogen bond mode.

Conclusions

In this study, multiple trajectories molecular dynamics simulation combined with MM-GBSA calculations were used to study the complex of zanamivir with neuraminidase of new strain 2009 influenza A (H1N1) virus. Different strains (including wide type, E119A/D, R152K, H275Y and R293K) were studied to identify potential drug resistance sites. Based on the results of MD simulation and MM-GBSA calculations, we found that zanamivir would be significantly resistant to the modeled mutants of the 2009-H1N1 strains except the H275Y mutant. According to the binding free energy, zanamivir will lose its effectiveness to the studied mutants in the following ranked order: R293K (-2.41 kcal mol^{-1})> R152K (-11.44 kcal mol^{-1})> E119D (-11.59 kcal mol^{-1})>E119A (-12.46 kcal mol^{-1}). The origin of resistance is mainly from the loss of polar interactions. This information indicates it is urgent and necessary to develop new and effective drugs to combat drug resistance mutants. This study can provide some useful insights for the rational design of the new effective medicine against the new resistant influenza strains.

Acknowledgments This work was supported by the National Natural Science Foundation of China (Grant No: 20905033) and the Fundamental Research Funds for the Central Universities (Grant No: lzujbky-2009-97). The authors also would like to thank the Gansu Computing Center for providing the computing resources.

References

1. Garten RJ, Davis CT, Russell CA et al (2009) Antigenic and genetic characteristics of swine-origin 2009 A (H1N1) influenza viruses circulating in humans. Science 325:197–201
2. CDC (2010) Antiviral Drugs and H1N1 Flu (Swine Flu). http://www.cdc.gov/h1n1flu/antiviral.htm. Accessed 10 July 2010)
3. Abed Y, Nehmé B, Baz M, Boivin G (2008) Activity of the neuraminidase inhibitor A-315675 against oseltamivir-resistant influenza neuraminidases of N1 and N2 subtypes. Antivir Res 77:163–166

4. Collins PJ, Haire LF, Lin YP, Liu J, Russell RJ, Walker PA, Skehel JJ, Martin SR, Hay AJ, Gamblin SJ (2008) Crystal structures of oseltamivir-resistant influenza virus neuraminidase mutants. Nature 453:1258–1261
5. Boivin G, Goyette N (2002) Susceptibility of recent Canadian influenza A and B virus isolates to different neuraminidase inhibitors. Antivir Res 54:143–147
6. Zürcher T, Yates PJ, Daly J, Sahasrabudhe A, Walters M, Dash L, Tisdale M, McKimm-Breschkin JL (2006) Mutations conferring zanamivir resistance in human influenza virus N2 neuraminidases compromise virus fitness and are not stably maintained in vitro. J Antimicrob Chemoth 58:723–732
7. Mishin VP, Hayden FG, Gubareva LV (2005) Susceptibilities of antiviral-resistant influenza viruses to novel neuraminidase inhibitors. Antimicrob Agents Chemoth 49:4515–4520
8. Arias CF, Escalera-Zamudio M, Soto-Del Río Mde L, Cobián-Güemes AG, Isa P, López S (2009) Molecular Anatomy of 2009 Influenza Virus A (H1N1). Arch Med Res 40:643–654
9. Gubareva LV, Webster RG, Hayden FG (2002) Detection of influenza virus resistance to neuraminidase inhibitors by an enzyme inhibition assay. Antivir Res 53:47–61
10. http://www.cdc.gov/mmwr/preview/mmwrhtml/mm5832a3.htm (accessed August 9, 2010)
11. Cao ZW, Han LY, Zheng CJ, Ji ZL, Chen X, Lin HH, Chen YZ (2005) Computer prediction of drug resistance mutations in proteins. Drug Discov Today 10:521–529
12. Chachra R, Rizzo RC (2008) Origins of resistance conferred by the R292K neuraminidase mutation via molecular dynamics and free energy calculations. J Chem Theor Comput 4:1526–1540
13. Hou T, McLaughlin WA, Wang W (2008) Evaluating the potency of HIV-1 protease drugs to combat resistance. Proteins 71:1163–1174
14. Zhang J, Hou T, Wang W, Liu JS (2010) Detecting and understanding combinatorial mutation patterns responsible for HIV drug resistance. Proc Natl Acad Sci USA 107:1321–1326
15. Srinivasan J, Cheatham TE, Cieplak P, Kollman PA, Case DA (1998) Continuum solvent studies of the stability of DNA, RNA, and phosphoramidate–DNA helices. J Am Chem Soc 120:9401–9409
16. Kollman PA, Massova I, Reyes C, Kuhn B, Huo S, Chong L, Lee M, Lee T, Duan Y, Wang W, Donini O, Cieplak P, Srinivasan J, Case DA, Cheatham TE (2000) Calculating structures and free energies of complex molecules: combining molecular Molecular mechanics and continuum models. Acc Chem Res 33:889–897
17. Tsui V, Case DA (2000) Theory and applications of the generalized born solvation model in macromolecular simulations. Biopolymers 56:275–291
18. Onufriev A, Bashford D, Case DA (2000) Modification of the generalized Born model suitable for macromolecules. J Phys Chem B 104:3712–3720
19. Feig M, Brooks CL (2002) Evaluating CASP4 predictions with physical energy functions. Proteins 49:232–245
20. Gourmala C, Luo Y, Barbault F, Zhang Y, Ghalem S, Maurel F, Fan B (2007) Elucidation of the LewisX–LewisX carbohydrate interaction with molecular dynamics simulations: A glycosynapse model. J Mol Struct THEOCHEM 821:22–29
21. Shaikh SA, Jayaram B (2007) A swift all-atom energy-based computational protocol to predict DNA-ligand binding affinity and $^{\triangle}T_m$. J Med Chem 50:2240–2244
22. Liu H, Yao X, Wang C, Han J (2010) In silico identification of the potential drug resistance sites over 2009 Influenza A (H1N1) virus neuraminidase. Mol Pharmaceutics 7:894–904
23. Rungrotmongkol T, Malaisree M, Nunthaboot N, Sompornpisut P, Hannongbua S (2010) Molecular prediction of oseltamivir efficiency against probable influenza A (H1N1-2009) mutants: molecular modeling approach. Amino Acids 39:393–398
24. DeLano WL (2002) The PyMOL Molecular Graphics System DeLano Scientific, Palo Alto, CA, USA. http://www.pymol.org
25. Li Q, Qi J, Zhang W, Vavricka CJ, Shi Y, Wei J, Feng E, Shen J, Chen J, Liu D, He J, Yan J, Liu H, Jiang H, Teng M, Li X, Gao GF (2010) The 2009 pandemic H1N1 neuraminidase N1 lacks the 150-cavity in its active site. Nat Struct Mol Biol 17:1266–1268
26. Case DA, Cheatham TE, Darden T, Gohlke H, Luo R, Merz KM, Onufriev A, Simmerling C, Wang B, Woods RJ (2005) The Amber biomolecular simulation programs. J Comput Chem 26:1668–1688
27. Duan Y, Wu C, Chowdhury S, Lee MC, Xiong G, Zhang W, Yang R, Cieplak P, Luo R, Lee T, Caldwell J, Wang J, Kollman PA (2003) A point-charge force field for molecular mechanics simulations of proteins based on condensed-phase quantum mechanical calculations. J Comput Chem 24:1999–2012
28. Lee MC, Duan Y (2004) Distinguish protein decoys by using a scoring function based on a new AMBER force field, short molecular dynamics simulations, and the generalized born solvent model. Proteins: Struct Funct Bioinform 55:620–634
29. Wang JM, Wolf RM, Caldwell JW, Kollman PA, Case DA (2004) Development and testing of a general amber force field. J Comput Chem 25:1157–1174
30. Jorgensen WL, Chandrasekhar J, Madura JD, Impey RW, Klein ML (1983) Comparison of simple potential functions for simulating liquid water. J Chem Phys 79:926–935
31. Berendsen HJC, Postma JPM, van Gunsteren WF, DiNola A, Haak JR (1984) Molecular dynamics with coupling to an external bath. J Chem Phys 81:3684–3690
32. Essmann U, Perera L, Berkowitz ML, Darden TA (1995) Smooth particle mesh Ewald method. J Chem Phys 103:8577–9593
33. Ryckaert JP, Ciccotti G, Berendsen HJC (1977) Numerical integration of the cartesian equations of motion of a system with constraints: molecular dynamics of n-alkanes. J Comput Phys 23:327–341
34. Sitkoff D, Sharp KA, Honig B (1994) Accurate calculation of hydration free energies using macroscopic solvent models. J Phys Chem 98:1978–1988
35. Case DA (1994) Normal mode analysis of protein dynamics. Curr Opin Struct Biol 4:285–290
36. Varghese JN, Smith PW, Sollis SL (1998) Drug design against a shifting target: a structural basis for resistance to inhibitors in a variant of influenza virus neuraminidase. Structure 6:735–746
37. Smith BJ, McKimm-Breshkin JL, McDonald M (2002) Structural studies of the resistance of influenza virus neuramindase to inhibitors. J Med Chem 45:2207–2212
38. McKimm-Breschkin J, Sahasrabudhe A, Blick T (2001) Mechanisms of resistance of influenza virus to neuraminidase inhibitors. Int Congress Series 1219:855–861
39. Chang CA, Chen W, Gilson MK (2007) Ligand configurational entropy and protein binding. Proc Natl Acad Sci USA 104:1534–1539
40. Gohlke H, Klebe G (2002) Approaches to the description and prediction of the binding affinity of small-molecule ligands to macromolecular receptors. Angew Chem Int Edn 41:2644–2676